Optical adaptive filtering for Doppler shift simulator*

HOU Jia-qing (侯佳庆)[1], **YAO Yuan** (姚远)[1], **LI Jin-ye** (李金野)[2], **LIU Hai-feng** (刘海锋)[1,2]**, **LIU Bo** (刘波)[1], **LIN Wei** (林炜)[1], **and ZHANG Hao** (张昊)[1]

1. *Tianjin Key Laboratory of Optoelectronic Sensor and Sensing Network Technology, Institute of Modern Optics, Nankai University, Tianjin 300350, China*
2. *The State Key Laboratory of Integrated Optoelectronics, Institute of Semiconductors, Chinese Academy of Sciences, Beijing 100083, China*

(Received 9 April 2019; Revised 11 May 2019)

Based on free space laser communication, this article describes the working principle of electro-optical frequency shifting, designs an optical adaptive filtering module, and builds the core module of the dynamic optical Doppler shifting simulator for laser channel. It is expected to be applied to the heaven-ground integrated communication link. In this article, we adopt the electro-optical frequency shifting technique combined with the microwave-light wave. In the 1 550 nm band, the negative feedback algorithm is used to complete the adaptive filtering, which realizes optical Doppler frequency shifting and high-precision locking. The frequency shift range reaches +5.5—+32 GHz, and the analog precision is better than 645 Hz. When the microwave frequency is greater than 13.5 GHz, the signal-to-noise ratio (*SNR*) of the output optical power reaches 20 dB, which lays the foundation for the next stage space laser communication.

Document code: A **Article ID:** 1673-1905(2019)05-0330-5

DOI https://doi.org/10.1007/s11801-019-9055-8

Compared with the traditional microwave communication, the free-space laser communication with laser beam as the carrier has high frequency, good spatial and temporal coherence and transmitting by beams, so it has high code rate, large communication capacity, small antenna size and low power consumption. These advantages help us construct a space-based broadband network and realize a high-speed integrated information network[1-3]. The communication system has been transitioned from direct probing communication to coherent demodulation with a communication rate of 5.6 Gbit/s[4,5]. The research in China has started relatively late, but it has also achieved fruitful results in recent years[6,7].

Space laser communication can adopt two kinds of communication modulation methods: direct detection and coherent detection. Laser coherent detection has higher receiving sensitivity and stronger background light suppression capability, and is the first choice for space system space laser link[8]. However, due to the high relative velocity and acceleration between satellites and between the stars, it will inevitably lead to a large optical carrier Doppler shift of the optical signal received by the laser terminal relative to the optical signal emitted from the source[9-11].

At present, there are mature ground demonstration verification test programs for laser modulation methods, rates, beam quality, and communication quality. However, how to simulate the optical carrier Doppler frequency shift in the ground system and perform the whole machine test of the communication system in this state is a difficult problem in the ground demonstration of the space laser communication system.

In this paper, a set of optical Doppler shifting frequency simulator is designed based on adaptive filtering module, which realizes large dynamic range and high precision laser Doppler simulation to meet the needs of spatial laser channel Doppler dynamic simulation verification.

The wavelength of the object's radiation changes due to the relative motion of the wave source and the observer, known as the Doppler effect[12]. The principle of Doppler shift is as shown in Fig.1. When the mobile station moves on the route of length d at a constant velocity v, the signal from the source S is received at the endpoints X and Y, and a frequency difference f_d is generated. We call it Doppler shift.

The distance difference between the radio wave starting from the source S and being received by the mobile station at point X and point Y is

$$\Delta l = d \cdot \cos\theta = v \cdot \Delta t \cdot \cos\theta \,. \tag{1}$$

* This work has been supported by the National Natural Science Foundation of China (No.61727815), and the Opened Fund of the State Key Laboratory of Integrated Optoelectronics (No.IOSKL2018KF18).

** E-mail: hfliu@nankai.edu.cn

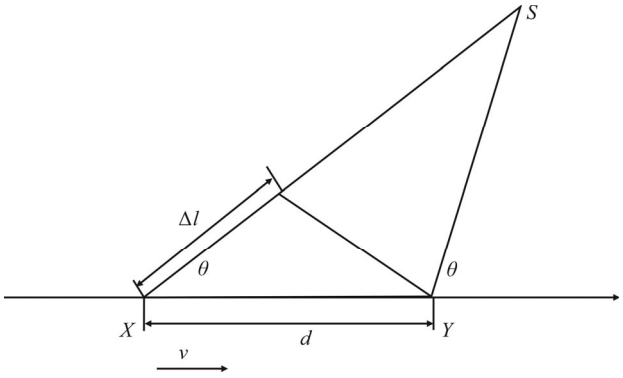

Fig.1 Doppler effect schematic

Due to the difference in distance, the phase change and frequency change of the received signal are

$$\Delta\varphi = \frac{2\pi\Delta l}{\lambda} = \frac{2\pi v\Delta t}{\lambda}\cos\theta \ , \tag{2}$$

$$f_d = \frac{1}{2\pi}\frac{\Delta\varphi}{\Delta t} = \frac{v}{\lambda}\cos\theta \ . \tag{3}$$

Therefore, when the receiving station and the wave source move relative to each other, the frequency of the receiving end changes.

In order to realize the Doppler dynamic simulation of the spatial laser channel, high-quality, wide-band, high-precision, and fast dynamic frequency shifting of the input laser signal is required to be achieved. Since the maximum frequency shift range of acousto-optic shifting is only 1 GHz, it is far from satisfying the bandwidth band required for the analog Doppler effect[13,14]. Therefore, the system uses electro-optical frequency shifting technology to achieve high spectral quality broadband laser frequency shifting.

The core of electro-optical frequency shifting technology is the electro-optic modulator[15,16]. Fig.2 is the Mach-Zehnder (MZM) electro-optic modulator's principle block diagram.

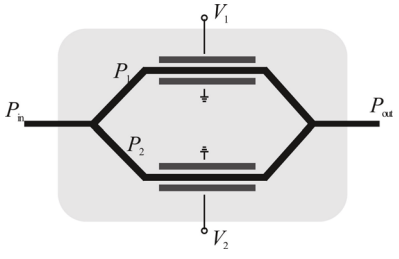

Fig.2 Principle diagram of the MZM electro-optic modulator

The MZM is composed of a two-arm $LiNbO_3$ crystal that achieves intensity or phase modulation of the output laser signal by applying different voltages across the arms. The system is driven by voltages of different frequencies to obtain various modulation sidebands relative to the input optical carrier, that is, frequency-shifted lasers[17].

The linewidth of the laser beam obtained after modulation is superimposed on the original line, and the linewidth of the microwave signal source is superimposed on the original basis. Therefore, the laser frequency shifting technology of MZM does not change the laser linewidth significantly, and the performance of the laser communication system will not be deteriorated. The sideband laser can be generated by the MZM electro-optic modulator, but the output spectrum also contains carrier light and other modulation order optical signals. In order to achieve the extraction of the frequency-shifted signal, the carrier signal of the electro-optic modulator must be suppressed.

The carrier suppression principle of the MZM modulator is as follows.

Assuming that the RF signal input is in the form of cosine, according to the intensity modulator formula:

$$\begin{aligned} E = {} & 2\cos\omega_c t\cdot\cos\left(\beta\cdot\cos\omega_m t+\phi_{DC}\right) = \\ & 2\cos\omega_c t\cdot[J_0(\beta)\cos(\phi_{DC})+ \\ & 2J_1(\beta)\cos\omega_m t\cdot\cos\left(\phi_{DC}+\frac{\pi}{2}\right)+ \\ & 2J_2(\beta)\cos 2\omega_m t\cdot\cos(\phi_{DC}+\pi)+\cdots]. \end{aligned} \tag{4}$$

Therefore, the modulator can be operated in the carrier suppression state by adjusting the ϕ_{DC}

$$\begin{aligned} & E\propto J_1(\beta)\cdot\cos\omega_c t\cdot\cos\omega_m t\propto \\ & J_1(\beta)\cdot\left[\cos(\omega_c+\omega_m)t+\cos(\omega_c-\omega_m)t\right]. \end{aligned} \tag{5}$$

After carrier suppression, the carrier is strongly suppressed, and the sideband laser signal is significantly enhanced.

Combined MZM, to eliminate the carrier signal and improve the *SNR*, a tunable narrowband fiber F-P filtering technique with a high extinction ratio is also needed to further enhance the required sideband signals while further suppressing the carrier signal.

The experimental diagram of the adaptive filtering system based on Doppler frequency shifting is shown in Fig.3. It mainly includes a 1 550 nm ultra-narrow linewidth laser (RIO Orion™), an MZM, a tunable microwave source, an FFP-TF2 tunable filter and an adaptive filter module, etc. The whole system of the experimental device adopts the polarization-maintaining fiber in the 1 550 nm band. The filter's free spectral range (*FSR*) is 8 nm (800 GHz), and the insertion loss is lower than 1.5 dB, the *FWHM* is better than 2 GHz (16 pm). The tunable microwave source has a frequency range of 0—32 GHz and a minimum step of 645 Hz with a frequency shift accuracy of 645 Hz. The core module is an adaptive filtering system. The system is based on STM32F103 chip, combined with photodetector, amplification module, A/D signal conversion and negative feedback module.

The optical adaptive filtering is based on negative feedback module algorithm, as shown in Fig.4. The single chip microcomputer drives the F-P filter, samples and peaks the filtered laser, and feeds back the driving

voltage corresponding to the shifted laser to the F-P filter. We set an adaptive condition that compares the sampled signal with the intensity of the previously filtered sideband. When the deviation is within 1 dB, it is considered to satisfy the adaptive condition. Sampling and judgment continue throughout the process, to ensure that adaptive conditions are met and self-tracking and locking of the desired sidebands is completed. When the laser is modulated, the adaptive processing module will control the drive voltage of the F-P filter to accurately track the lock and filter out the desired sideband laser.

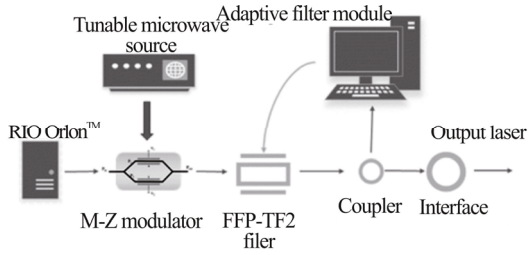

Fig.3 Adaptive filtering system for Doppler frequency shift

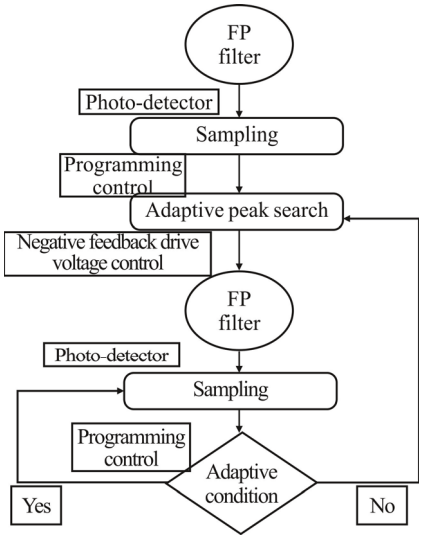

Fig.4 Adaptive peak search algorithm process

The detail process of adaptive peak search is described as following.

Firstly, a sawtooth wave is applied to drive the F-P filter to sample the spectrum of laser. Thanks to the narrowband of F-P filter, assisted with a single photodetector, the spectrum of the modulated laser can be measured and saved in an array.

Then, an algorithm is used to detect the peaks of the array. Because the intensities of the high order sidebands are very low, three peaks as well as their drive voltages in the array can be detected, which corresponds to carrier and ±1st order sidebands. Peaks search is achieved.

Furthermore, we drive the F-P filter by the detected voltage to the target peak. To monitor and track the filter at this peak, we drive the F-P filter to sample around this peak. As long as the adaptive condition is not satisfied, the feedback will drive the F-P filter to a new round peak search. Then, adaptive peak search is achieved. It is worth pointing out that, due to the narrow bandwidth of F-P filter, the other sidebands and the carrier can be filtered in peaking search process. So, the optical adaptive filtering is achieved at the same time of adaptive peak search.

In the 1 550 nm band, the frequency shift of 1 GHz corresponds to a wavelength drift of 0.008 nm. After 17.5 GHz frequency shift, the primary sideband drifts by 0.14 nm compared to the carrier.

The spectrum of the laser is shown in Fig.5. The spectrometer model is AQ6370C with a minimum wavelength resolution of 0.02 nm and an intensity resolution of −80 dBm. The center wavelength is 1 549.688 nm. The experimentally measured optical power is −22.631 dBm due to coupling and other losses.

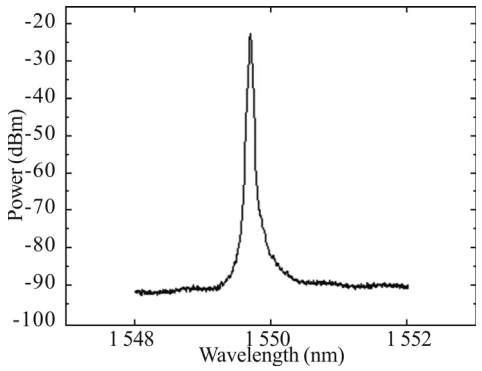

Fig.5 Laser spectrum

As shown in Fig.6, the initial frequency of the tunable microwave source is set to 17.5 GHz, which is the modulating signal, and the output laser is modulated by an electro-optic intensity modulator to produce various modulation sideband. As shown in Eqs.(4) and (5), the cosine modulation of the intensity can be expanded as the sum of a series of Bessel functions with different orders, which corresponds to the sidebands of the modulated light. The first peaks at two sides of the, i.e. peak 0, are ±1 order sidebands respectively. The other peaks are higher order sidebands, including ±2, ±3 etc. Controlling the modulator driving voltage to change Φ_{DC} can reduce the carrier intensity and increase the intensity of the first-order sideband, and output the modulated laser after carrier suppression. As shown in the spectrum: after the carrier is modulated, the wavelength is unchanged at 1 549.688 nm and the intensity is −34.478 dBm; the −1 sideband has a wavelength of 1 549.548 nm and an intensity of −37.075 dBm; the +1 sideband's wavelength is 1 549.828 nm and its intensity is −36.505 dBm. Since the laser is not an ideal narrow linewidth laser, the positive and negative level 1st sidebands in Fig.6 are not completely symmetrical.

In order to get the laser at the desired frequency, we need to use an adaptive filtering system to take out the modulated laser sideband. As shown in Fig.7, when the

microwave frequency is 17.5 GHz, the filtered +1-order sideband intensity is −40.47 dBm, the carrier intensity is −59.585 dBm, and the *SNR* is 19.115 dB. Obviously, the Doppler shift signal can be well simulated.

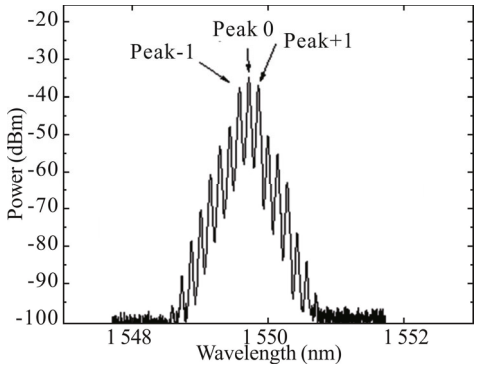

Fig.6 Intensity-modulated laser spectrum

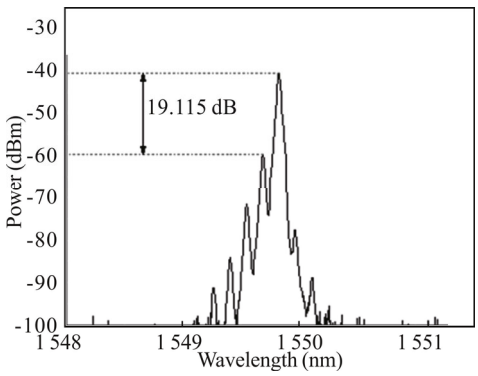

Fig.7 17.5G fixed frequency filter spectrum

Fig.8 shows the red-shifted adaptive filtering spectra under different modulation frequencies. Only the microwave source is adjusted to change the microwave modulated signal loaded on the carrier. In order to test the frequency shift range, we adjust the microwave frequency from 17.5 GHz to 32 GHz. Fig.8 shows that the spectra of the tunable microwave source gradually changes from 17.5 GHz to 32 GHz. The minimum step size of the microwave source is 645 Hz. The frequency of the tunable microwave source is gradually changed by the computer. After many experiments, the adaptive system is able to self-track the +1st sideband and filter out the required frequency-shifted laser with an *SNR* of 20 dB. As shown in Eq.(4), in the first modulation period, the microwave source frequency ω_m is gradually increased, and the $\cos(\omega_m)$ in the 1st-order modulated light is decreased, and the power of the modulated light is gradually decreased. The intensity of the +1-order sideband decreases as the modulation frequency of the microwave source increases, which is described in this figure.

Fig.9 shows the blue-shifted adaptive filtering spectra under different modulation frequencies. Only the microwave source is adjusted to reduce the modulation signal from 17.5 GHz to 4.5 GHz, to reduce the frequency shifting bandwidth. As shown in this figure, when the modulation frequency is reduced to 13.5 GHz, the *SNR* of the frequency-shifted laser to the carrier is still 20 dB; when the microwave frequency continues to decrease to 9.5 GHz, the *SNR* is gradually reduced to 15 dB; when the microwave frequency is lowered to 5.5 GHz, the *SNR* of the +1-level sideband to the carrier is only 10 dB. Laser pulses are heavily overlapped.

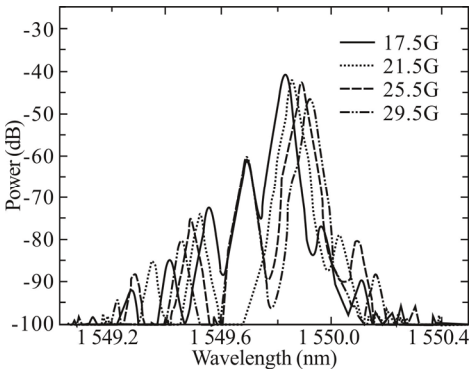

Fig.8 Red-shifted adaptive filtering spectra under different modulation frequencies

The reasons for this phenomenon are that the *FWHM* of the F-P filter is 2 GHz and the edge of the F-P filter is not a complete rectangle, but a high-slope trapezoidal edge. Therefore, when the +1st sideband of the output laser is close to the carrier's frequency, the *SNR* of the frequency-shifted laser filtered by the F-P filter is gradually reduced.

In order to solve the problem of the low *SNR* in low frequency bandwidth range, a dual-shift scheme can be adopted. A fixed microwave source and a fixed wavelength filter are used both in the first frequency shifting. The frequency of the fixed microwave source is 17.5 GHz. After the frequency-shifted laser is amplified by erbium-doped fiber amplifier (EDFA), the tunable microwave source with a frequency shift range of 0—32 GHz can be used to shift the frequency in the opposite direction to obtain a frequency-shifted laser with a lower frequency shift range. At this scheme, the *SNR* of the frequency-shifted signal in the low frequency band range is same as that in the high frequency direction.

Fig.10 shows the filtering accuracy of the adaptive filtering system. As the modulation frequency of the microwave source changes, the adaptive filtering system will filter out the +1st harmonic of the corresponding wavelength. We use software to fit, the result is a linear function, Y is the +1st harmonic's wavelength (nm), X is the microwave source modulation frequency (GHz), and the formula is fitted to

$$Y=1\ 549.687\ 21+0.007\ 86X. \quad (6)$$

Its correlation coefficient is 0.999 78, showing good linearity. The slope is 0.007 86, which means that the

frequency shift accuracy is 0.007 86 nm/GHz, which is consistent with the theoretical value of 0.008 009 nm/GHz. It proves the stability and accuracy of the adaptive filtering system in the frequency shift experiment.

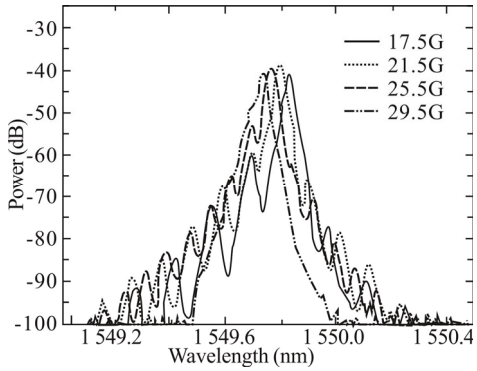

Fig.9 Blue-shifted adaptive filtering spectra under different modulation frequencies

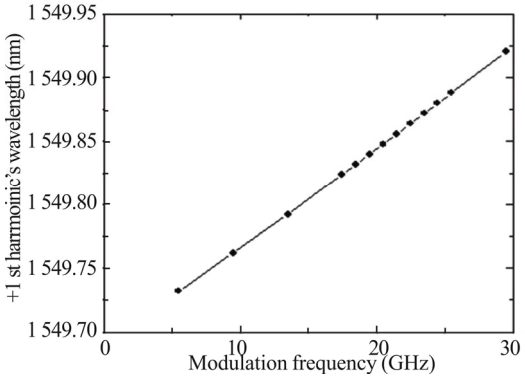

Fig.10 Filtering accuracy of the adaptive filtering system

In summary, for the free-space laser communication ground demonstration and verification system, the problem of Doppler frequency shift of optical carrier can not be simulated. A set of adaptive filtering system based on Doppler frequency shift is designed and constructed. This experiment analyzes and verifies the frequency shift performance of the Doppler shift frequency simulator used for terrestrial demonstration. The experimental results show that the filter range of the optical adaptive filtering module is 5.5—32 GHz in total (5.5—17.5 GHz and 17.5—32 GHz). When a laser with an input optical power of −22 dBm is used as the carrier, after splitting and coupling, the laser power after shifting is greater than −40 dBm and the frequency shift accuracy reaches 0.007 86 nm/GHz. When the frequency shift frequency is greater than 13.5 GHz, the filtered frequency-shifted laser has an *SNR* of 20 dB. To get a lower frequency shift range of the laser, a dual frequency-shifted scheme can be used.

The optical adaptive filtering system based on Doppler frequency shift can solve the technical problem that the ground demonstration and verification system in space laser communication can't accurately estimate and compensate the Doppler frequency shift, and it has broad application prospects.

References

[1] Sodnik Zoran, Smit Hans, Sans Marc, Zayer Igor, Lanucara Marco, Montilla Iciar and Alonso Angel, LLCD Operations Using the Lunar Lasercom OGS Terminal, Free-Space Laser Communication and Atmospheric Propagation XXVI 8971, 89710W (2014).

[2] Yu Siyuan, Bao Fangdi, Wu Feng, Li Mengnan and Ma Jing, Research on Adaptive Compensation Techniques in Laser Communication Links, 2015 Fifth International Conference on Instrumentation and Measurement, Computer, Communication and Control (IMCCC), 43 (2015).

[3] Neumann G, Cavanaugh Jf, Coyle Db, Mcgarry J, Smith D, Sun X, Torrence M, Zagwodski Tw and Zuber Mt, Laser Ranging at Interplanetary Distances, Proc. 15th International Workshop on Laser Ranging, Canberra, Australia, 2006.

[4] Huilin Jiang, Yan An, Yalin Zhang, Lun Jiang and Yiwu Zhao, Journal of Spacecraft Measurement and Control **34**, 207 (2015). (in Chinese)

[5] Kikuchi Toru, Koretsune Takashi, Arita Ryotaro and Tatara Gen, Physical Review Letters **116**, 247201 (2016).

[6] Fen Wu, Siyuan Yu, Zhongtian Ma, Jing Ma and Liyin Tan, Chinese Journal of Lasers **40**, 0605008-1 (2014).

[7] Hao Qi, Ma Jing and Tan Liying, Standing on the Top of the World of Satellite Laser Communication, 2017. (in Chinese)

[8] Jing Dong, Rui Chen, Xiaolong Li and Jun Zhang, Chinese Journal of Lasers **39**, 199 (2012). (in Chinese)

[9] Haili Cui and Shoufeng Zhai, Science & Technology Information **15**, 26 (2017). (in Chinese)

[10] Vercesi Valeria, Onori Daniel, Laghezza Francesco, Scotti Filippo, Bogoni Antonella and Scaffardi Mirco, Optics Letters **40**, 1358 (2015).

[11] Mouche Alexis A, Collard Fabrice, Chapron Bertrand, Dagestad Knut-Frode, Guitton Gilles, Johannessen Johnny A, Kerbaol Vincent and Hansen Morten Wergeland, IEEE Transactions on Geoscience and Sensing Remote **50**, 2901 (2012).

[12] Drain Leslie E J Chichester, The Laser Doppler Techniques, Sussex, England and New York Wiley-Interscience, 250 (1980).

[13] Liren Guo, Yihua Hu and Zheng Li, Acta Optica Sinica **35**, 200 (2015). (in Chinese)

[14] Kim Byoung Yoon, Blake Jn, Engan He and Shaw H, Optics Letters **11**, 389 (1986).

[15] Buhrer CF, Baird D and Conwell EM, Applied Physics Letters **1**, 46 (1962).

[16] Jianmo Lu, Weinan Wang and Yanhe Li, Acta Optica Sinica **27**, 159 (2007). (in Chinese)

[17] Qin He, Research on Advanced Modulation Technology Based on MZM in WDM-PON, Xi'an University of Posts and Telecommunications, 2013. (in Chinese)